15-Deoxy-$\Delta^{12,14}$-prostaglandin J_2 induces growth inhibition, cell cycle arrest and apoptosis in human endometrial cancer cell lines

HAILI LI[1,2] and HISASHI NARAHARA[1]

[1]Department of Obstetrics and Gynecology, Oita University Faculty of Medicine, Yufu-shi, Oita, Japan;
[2]Department of Obstetrics and Gynecology, The Fourth Hospital of Hebei Medical University, Shijiazhuang, Hebei, P.R. China

Received November 3, 2012; Accepted January 7, 2013

DOI: 10.3892/ijmm.2013.1268

Abstract. 15-Deoxy-$\Delta^{12,14}$-prostaglandin J_2 (15d-PGJ_2), a peroxisome proliferator-activated receptor γ ligand, has been reported to have antiproliferative activity in certain types of cancer. The purpose of this study was to elucidate the effect of 15d-PGJ_2 on endometrial cancer cells, as well as the mechanism of action. Endometrial cancer-derived cells (HHUA, Ishikawa and HEC-59) were treated with various concentrations of 15d-PGJ_2, and its effects on cell growth, the cell cycle and apoptosis were investigated *in vitro*. Using cDNA microarrays, some potential targets of this drug were identified. All endometrial cancer cell lines were sensitive to the growth-inhibitory effect of 15d-PGJ_2. Cell cycle arrest at the G2/M phase of the cell cycle and induction of apoptosis were observed. Concerning the gene expression changes induced by 15d-PGJ_2 treatment, the upregulation of aldo-keto reductase family 1 member C3 (AKR1C3) and the downregulation of anterior gradient homolog 3 (AGR3) and nitric oxide synthase 2A (NOS2A) were confirmed using western blot analysis in all the cell lines examined. These results suggest that 15d-PGJ_2 may be a novel therapeutic option for the treatment of endometrial cancer.

Introduction

Endometrial cancer is the most common malignant tumor of the female genital tract, and its incidence has increased in recent years (1,2). Furthermore, the search for agents effective in the treatment of either advanced or recurrent endometrial cancer has proved to be disappointing (2,3). Therefore, innovative approaches are required for the treatment of endometrial cancer.

Peroxisome proliferator-activated receptor (PPAR)γ is a nuclear hormone receptor and its ligands, troglitazone and pioglitazone, have been shown to induce apoptosis in several types of cancer cells, including endometrial cancer cells (4-6). 15-Deoxy-$\Delta^{12,14}$-prostaglandin J_2 (15d-PGJ_2) is a PPARγ ligand that activates PPARγ at micromolar concentrations in humans *in vivo* (7-9). Recently, 15d-PGJ_2 was reported to have antiproliferative activity in certain types of cancer (4,10-12). However, the effect of 15d-PGJ_2 on endometrial cancer cells has not yet been investigated.

The present study aimed to investigate the biological and therapeutic effects of 15d-PGJ_2 on endometrial cancer. We examined whether this compound can mediate cell growth inhibition, cell cycle arrest and apoptosis in endometrial cancer cell lines (HHUA, Ishikawa and HEC-59). Furthermore, to identify potential and novel target genes responsive to the anticancer effect in 15d-PGJ_2-treated endometrial cancer cells, we analyzed the global changes in gene expression in HHUA cells following treatment with 15d-PGJ_2 using cDNA microarrays. The expression of candidate proteins was confirmed by western blot analysis in the 3 endometrial cancer cell lines.

Materials and methods

Cell lines. The HHUA human endometrial cancer cell line was obtained from Riken (Ibaraki, Japan). The Ishikawa human endometrial cancer cell line was kindly provided by Dr Masato Nishida (Tsukuba University, Ibaraki, Japan). The HEC-59 human endometrial cancer cell line was obtained from the American Type Culture Collection (Manassas, VA, USA). The cells were maintained as monolayers at 37˚C in 5% CO_2/air in Dulbecco's modified Eagle's medium (DMEM; Gibco, Rockville, MD, USA) containing 10% heat-inactivated fetal bovine serum (FBS; Omega, Tarzana, CA, USA).

Chemicals. 15d-PGJ_2 was obtained from Enzo Life Sciences (Plymouth Meeting, Montgomery County, PA, USA), and prepared as a 20 mg/ml stock solution in dimethyl sulfoxide (DMSO). The stock solution was stored in aliquots at -20˚C.

Assessment of cell proliferation and cell viability. The cell proliferation and cell viability were determined in 96-well plates by a modified methylthiazol tetrazolium (MTT) assay using WST-1 (Roche Diagnostics, Penzberg, Germany) following the manufacturer's instructions. We distributed $5x10^3$ cells in DMEM supplemented with 10% FBS into each well of a 96-well flat-bottomed microplate (Corning, Inc., New York, NY, USA) and incubated them overnight. The medium was then removed,

Correspondence to: Professor Hisashi Narahara, Department of Obstetrics and Gynecology, Oita University Faculty of Medicine, 1-1 Idaigaoka, Hasama-machi, Yufu-shi, Oita 879-5593, Japan
E-mail: naraharh@oita-u.ac.jp

Key words: 15-deoxy-$\Delta^{12,14}$-prostaglandin J_2, cell cycle, apoptosis, microarray, endometrial cancer

and the cells were incubated for 48 h with 100 μl of experimental medium containing various concentrations of 15d-PGJ$_2$. Thereafter, 10 μl of WST-1 dye was added to each well, and the cells were further incubated for 4 h. All experiments were performed in the presence of 10% FBS. Cell proliferation was evaluated by measuring the absorbance at 540 nm. Data were calculated as the ratio of the values obtained for the 15d-PGJ$_2$-treated cells to those for the untreated controls.

Cell cycle analysis by flow cytometry. The cell cycle was analyzed by flow cytometry after 2 days of culturing. Cells ($5x10^4$) were exposed to 15d-PGJ$_2$ in 6-well flat-bottomed plates for 48 h. Analysis was performed immediately after staining using the CellFIT program (Becton-Dickinson, San Jose, CA, USA), whereby the S phase was calculated using an RFit model.

Measurement of apoptosis [flow-cytometric analysis with the Annexin V/propidium iodide (PI) assay]. Cells were plated and grown overnight until they reached 80% confluence and then treated with 15d-PGJ$_2$. After 48 h, detached cells in the medium were collected, and the remaining adherent cells were harvested by trypsinization. The cells ($1x10^5$) were washed with PBS and resuspended in 250 μl of binding buffer (Annexin V-FITC kit; Becton-Dickinson) containing 10 μl of 20 μg/ml PI and 5 μl of Annexin V-FITC, which binds to phosphatidylserine translocated to the exterior of the cell membrane early in the apoptotic pathway as well as during necrosis. After incubation for 10 min at room temperature in a light-protected area, the samples were analyzed on a FACSCalibur flow cytometer (Becton-Dickinson). FITC and PI emissions were detected in the FL-1 and FL-2 channels, respectively. For each sample, data from 30,000 cells were recorded in list mode on logarithmic scales. Subsequent analysis was performed with CellQuest software (Becton-Dickinson).

Mitochondrial transmembrane potential (MTP). Cells were prepared for FACS analysis as described above and stained using a Mitocapture Apoptosis Detection kit obtained from BioVision (Palo Alto, CA, USA) with a fluorescent lipophilic cationic reagent that assesses mitochondrial membrane permeability, according to the manufacturer's recommendations.

Microarray analysis. Total RNA was extracted from the 15d-PGJ$_2$-treated and untreated HHUA cells using an RNeasy mini kit (Qiagen, Valencia, CA, USA) in accordance with the manufacturer's instructions. Prior to hybridization, the quantity and quality of the total RNA were evaluated using a spectrophotometer and a 2100 Bioanalyzer (Agilent Technologies, Santa Clara, CA, USA), respectively. Cy3-labeled cRNA targets were generated using a Low RNA Input Fluorescent Linear Amplification kit (Agilent Technologies). A human 44 K oligoarray was used for hybridization, in accordance with the manufacturer's recommendations (Agilent Technologies). A laser confocal scanner (Agilent Technologies) was used to measure signal intensities in the expression microarray analysis. Feature Extraction software (Version 9.1; Agilent Technologies) with the manufacturer's recommended settings was applied for the microarray image analysis. Analysis of the microarray images was performed with GeneSpring 7.3.1 software (Agilent Technologies). For comparison among multiple arrays, probe set data were median-normalized/chip. The data were then centered across the genes in 6 normal controls, followed by filtering based on a signal intensity of ≥100, and contained no flagged values. Among these differentially expressed genes, those designated as 'upregulated' were overexpressed >2-fold in comparison with the controls ($P<0.05$), whereas those designated as 'downregulated' were underexpressed <0.75-fold compared with the controls ($P<0.05$). Annotations including chromosomal loci were provided by Agilent Technologies.

For Gene Ontology (GO) analysis, differentially expressed genes were defined as those with a >2-fold increase or decrease in expression relative to the controls. GO term enrichment in the upregulated or downregulated gene sets was assessed using the GOstat web tool (13).

Western blot analysis. Cells were washed twice in PBS, suspended in lysis buffer [50 mM Tris (pH 8.0), 150 mM NaCl, 0.1% SDS, 0.5% sodium deoxycholate, 1% NP-40, phenylmethylsulfonyl fluoride at 100 μg/ml, aprotinin at 2 μg/ml, pepstatin at 1 μg/ml and leupeptin at 10 μg/ml], and placed on ice for 30 min. After centrifugation at 15,000 x g for 15 min at 4˚C, the suspension was collected. Protein concentrations were quantified using the Bio-Rad protein Assay Dye Reagent Concentrate (Bio-Rad Laboratories, Hercules, CA, USA) according to the manufacturer's recommendations. Whole-cell lysates (40 μg) were resolved by SDS-polyacrylamide gel electrophoresis on a 4-15% gel, transferred onto a polyvinylidene difluoride membrane (Immobilon; Amersham, Arlington Heights, IL, USA), and probed sequentially with antibodies against anterior gradient homolog 3 (AGR3; 1:1,000; GeneTex, Irvine, CA, USA), aldo-keto reductase family 1 member C1 (AKR1C1; 1:1,000; GeneTex), aldo-keto reductase family 1 member C3 (AKR1C3; 1:1,000; ProteinTech, Chicago, IL, USA), α-1-microglobulin/bikunin precursor (AMBP; 1:1,000; Abnova, Taipei, Taiwan), complement component 3a receptor 1 (C3AR1; 1:1,000; Abnova), chondroadherin (CHAD; 1:1,000; Avia Systems Biology, San Diego, CA, USA), Fer3-like (*Drosophila*) (FERDL3; 1:1,000; Avia Systems Biology), ferritin, light polypeptide (FTL; 1:1,000; GeneTex), galactose-3-*O*-sulfotransferase 3 (GAL3ST3; 1:1,000; Avia Systems Biology), glutamate-cysteine ligase, modifier subunit (GCLM; 1:1,000; Abnova), heme oxygenase (decycling) 1 (HMOX1; 1:1,000; Abnova), intercellular adhesion molecule 4 (ICAM4; 1:1,000; Abnova), potassium voltage-gated channel, shaker-related subfamily, β member 1 (KCNAB1; 1:1,000; Osenses, Keswick, Australia), mitochondrial ribosomal protein L37 (MRPL37; 1:1,000; ProteinTech), nitric oxide synthase 2A (NOS2A; 1:1,000; Applied Biological Materials, Kampenhout, Belgium), phosphorylated eukaryotic translation initiation factor 4E (p-eIF4E; 1:1,000; Bioworld Technology, Minneapolis, MN, USA), pirin (PIR; 1:1,000; Avia Systems Biology), tripartite motif-containing 16 (TRIM16; 1:1,000; Avia Systems Biology), thioredoxin reductase 1 (TXNRD1; 1:1,000; ProteinTech), UDP glucuronosyltransferase 1 family, polypeptide A6 (UGT1A6; 1:1,000; LifeSpan Biosciences, Seattle, WA, USA) and GAPDH monoclonal antibody (mAb) (1:10,000; Santa Cruz Biotechnology, Inc., Santa Cruz, CA, USA). The blots were developed using an enhanced chemiluminescent (ECL) kit (Amersham). Band intensity was measured using the public domain Image program ImageJ version 1.44, and fold increase in expression as compared with control, untreated cells was calculated.

Table I. Cell cycle changes in endometrial cancer cell lines.

Cell line	Vehicle	15d-PGJ_2 (10 μM)
Ishikawa		
Sub G0/G1 (%)	3.1±0.1	6.2±0.3[a]
G0/G1 (%)	53.4±12.4	35.0±17.7[a]
S (%)	36.1±5.6	38.4±7.5
G2/M (%)	10.5±7.7	26.6±11.8[a]
HEC-59		
Sub G0/G1 (%)	2.7±0.1	0.5±0.1[a]
G0/G1 (%)	51.9±0.8	54.7±0.9
S (%)	35.8±0.6	31.6±1.2
G2/M (%)	12.3±0.3	13.6±0.7[a]
HHUA		
Sub G0/G1 (%)	3.9±0.8	5.2±2.0[a]
G0/G1 (%)	53.5±3.6	44.0±8.1
S (%)	35.3±1.7	44.0±4.0
G2/M (%)	11.3±2.0	12.1±4.0

Cells were plated in 15d-PGJ_2 wells and grown for 2 days, and cell cycle distribution was measured. Means ± SD are shown. [a]P<0.05 compared to the vehicle.

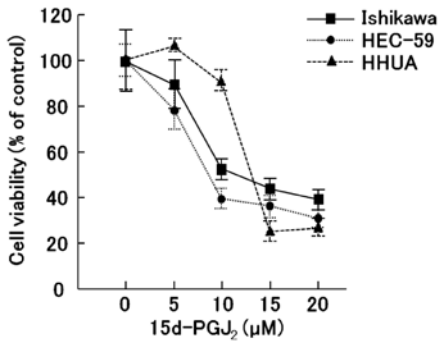

Figure 1. Effect of 15d-PGJ_2 on the growth of endometrial cancer cells *in vitro*. Ishikawa, HEC-59 and HHUA endometrial cancer cells were treated with either 15d-PGJ_2 at various concentrations (5-20 μM) or the dilutant (control) for 48 h, and cell growth (% of control) was measured using an WST-1 assay. Results represent the means ± SD of 3 independent experiments with triplicate dishes.

Table II. Cell death measured by Annexin V and mitochondrial transmembrane potential assay in endometrial cancer cell lines.

Assay/cell line	Vehicle	15d-PGJ_2 (10 μM)
Annexin V assay		
Ishikawa		
Viable (LL) (%)	92.5±0.1	48.4±1.6[a]
Apoptosis (LR) (%)	4.9±0.1	35.8±0.8[a]
Necrosis (UR) (%)	2.5±0.2	15.3±0.8[a]
HEC-59		
Viable (LL) (%)	86.7±0.3	56.3±1.0[a]
Apoptosis (LR) (%)	4.7±0.3	6.5±0.3
Necrosis (UR) (%)	5.4±0.1	16.7±0.4[a]
HHUA		
Viable (LL) (%)	79.2±8.5	61.9±5.9[a]
Apoptosis (LR) (%)	6.7±1.1	12.9±3.3[a]
Necrosis (UR) (%)	4.6±1.1	17.1±4.3[a]
MTP assay		
Ishikawa		
Viable (%)	76	44
Apoptosis (%)	25	59
HEC-59		
Viable (%)	77	58
Apoptosis (%)	23	44
HHUA		
Viable (%)	68	14
Apoptosis (%)	34	87

Induction of apoptosis by15d-PGJ_2 in endometrial cancer cells detected by Annexin V-FITC and PI staining (Annexin V assay). Cells were cultured with 10 μM of 15d-PGJ_2 for 48 h, stained with Annexin V-FITC and PI, and analyzed by flow cytometry. Each experiment was repeated 3 times. Data represent the means ± SD. LL, lower left quadrant (percentage of viable cells); LR, lower right quadrant (early apoptotic cells); UR, upper right quadrant (secondary necrotic cells). [a]P<0.05 compared to the vehicle. Effect of 15d-PGJ_2 treatment on the mitochondrial transmembrane potential (MTP assay). Cells were cultured with 10 μM of 15d-PGJ_2 for 48 h, and the MitoCapture intensity (representing MTP) was determined by flow cytometry.

Statistical analysis. Data are presented as the means ± SD of representative experiments and were analyzed by the Bonferroni-Dunn test using StatView 4.5 software (Abacus Concepts, Berkeley, CA, USA). A P-value <0.05 was considered to indicate a statistically significant difference.

Results

Effects of 15d-PGJ_2 on the proliferation and viability of endometrial cancer cell lines in vitro. The antitumor effects of 15d-PGJ_2 on 3 endometrial cancer cell lines *in vitro* were examined using a WST-1 assay of the 2-day exposure to 15d-PGJ_2. Significant inhibitory effects of 15d-PGJ_2 on the cell growth were observed in all 3 endometrial cancer cell lines (Ishikawa, HHUA and HEC-59) (Fig. 1).

Cell cycle analysis of endometrial cancer cells following exposure to 15d-PGJ_2. We then investigated whether 15d-PGJ_2 would lead to the induction of apoptosis and/or cell cycle arrest in the endometrial cancer cells (Table I). 15d-PGJ_2 led to an increase in the sub G0/G1 apoptotic cell population and the cell population in the G2/M phase of the cell cycle compared to treatment with the vehicle alone, with a concomitant decrease in the proportion of cells in the S phase.

Apoptotic changes in endometrial cancer cells treated with 15d-PGJ_2. To assess the ability of the endometrial cancer cells to undergo apoptosis in response to 15d-PGJ_2 exposure and to distinguish between the different types of cell death, we double-stained the 15d-PGJ_2-treated cells with Annexin V and PI and analyzed the results using flow cytometry. Annexin V

Table III. Upregulated genes following treatment with 15d-PGJ_2 in HHUA cells.

Fold changes	Gene symbol	Description	GenBank	UniGene	Map
17.50674	AKR1C1	Aldo-keto reductase family 1, member C1 (dihydrodiol dehydrogenase 1; 20-α (3-α)-hydroxysteroid dehydrogenase)	NM_001353	Hs.460260	10p15-p14
15.647071	AKR1C3	Aldo-keto reductase family 1, member C3 (3-α hydroxysteroid dehydrogenase, type II)	NM_003739	Hs.78183	10p15-p14
6.0476165	AMBP	α-1-microglobulin/bikunin precursor	NM_001633	Hs.436911	9q32-q33
5.751939	HMOX1	Heme oxygenase (decycling) 1	NM_002133	Hs.517581	22q12
4.723847	A_32_P157671				17p11.2
4.683617	TRIM16	Tripartite motif-containing 16	NM_006470	Hs.123534	17p11.2
4.5855446	PIR	Pirin (iron-binding nuclear protein)	NM_003662	Hs.495728	Xp22.2
4.380505	UGT1A6	UDP glucuronosyltransferase 1 family, polypeptide A6	NM_001072	Hs.654499	2q37
4.2928677	TXNRD1	Thioredoxin reductase 1	NM_003330	Hs.654922	12q23-q24.1
3.9529867	GCLM	Glutamate-cysteine ligase, modifier subunit	NM_002061	Hs.315562	1p22.1
3.817845	ENST00000313481				19p13.3
3.6058688	FTL	Ferritin, light polypeptide	NM_000146	Hs.433670	19q13.3-q13.4
3.4976888	CR598364	Full-length cDNA clone CS0CAP007YJ17 of Thymus of *Homo sapiens* (human)	CR598364	Hs.596052	
3.4703205	G6PD	Glucose-6-phosphate dehydrogenase	NM_000402	Hs.461047	Xq28
3.410493	SRXN1	Sulfiredoxin 1 homolog (*S. cerevisiae*)	NM_080725	Hs.516830	20p13
3.343625	SPP1	Secreted phosphoprotein 1 (osteopontin, bone sialoprotein I, early T-lymphocyte activation 1)	NM_000582	Hs.313	4q21-q25
3.3256302	A_24_P281683				11q23.3
3.108579	TXNRD1	Thioredoxin reductase 1	BG001037	Hs.654922	12q23-q24.1
3.0549212	PFKFB3	6-Phosphofructo-2-kinase/fructose-2,6-biphosphatase 3	NM_004566	Hs.195471	10p14-p15
3.0234468	FLJ35767	FLJ35767 protein	NM_207459	Hs.231897	17q25.3
2.9421628	EPHX1	Epoxide hydrolase 1, microsomal (xenobiotic)	NM_000120	Hs.89649	1q42.1
2.833596	GCNT3	Glucosaminyl (N-acetyl) transferase 3, mucin type	NM_004751	Hs.194710	15q21.3
2.699825	OSGIN1	Oxidative stress induced growth inhibitor 1	NM_013370	Hs.128055	16q23.3
2.6840672	GSR	Glutathione reductase	BC035691	Hs.271510	8p21.1
2.6485877	IKBKG	Inhibitor of κ light polypeptide gene enhancer in B-cells, kinase γ	NM_003639	Hs.43505	Xq28
2.6185443	ENST00000313774	*Homo sapiens* glucosaminyl (N-acetyl) transferase 3, mucin type, mRNA (cDNA clone MGC:9086 IMAGE:3851937), complete cds. [BC017032]		Hs.194710	15q22.2
2.5760007	DDC	Dopa decarboxylase (aromatic L-amino acid decarboxylase)	NM_000790	Hs.359698	7p11
2.5224981	LMNB1	Lamin B1	NM_005573	Hs.89497	5q23.3-q31.1
2.5161438	A_32_P7974				1q21.3
2.505143	NADSYN1	NAD synthetase 1	AL512694	Hs.556986	11q13.4
2.4961286	HSPA1A	Heat shock 70 kDa protein 1A	NM_005345	Hs.520028	6p21.3

Table III. Continued.

Fold changes	Gene symbol	Description	GenBank	UniGene	Map
2.47789	GCLC	Glutamate-cysteine ligase, catalytic subunit	NM_001498	Hs.654465	6p12
2.361285	CN272797	17000600009278 GRN_PREHEP *Homo sapiens* cDNA 5', mRNA sequence.	CN272797		9p23
2.3579373	HSPA8	Heat shock 70 kDa protein 8	BU731317	Hs.180414	11q24.1
2.3155344	C16orf28	Chromosome 16 open reading frame 28	NM_023076	Hs.643536	16p13.3
2.2990816	ABCB6	ATP-binding cassette, sub-family B (MDR/TAP), member 6	NM_005689	Hs.107911	2q36
2.2683835	ALDH3A2	Aldehyde dehydrogenase 3 family, member A2	NM_000382	Hs.499886	17p11.2
2.2379045	ENST00000238571	*Homo sapiens* (clone zap3) mRNA, 3' end of cds. [L40403]		Hs.531111	14q24.3
2.2241304	GLA	Galactosidase, α	NM_000169	Hs.69089	Xq22
2.2137868	PRDX1	Peroxiredoxin 1	NM_002574	Hs.180909	1p34.1
2.2122195	ANGPTL4	*Homo sapiens* angiopoietin-like 4 (ANGPTL4), transcript variant 2, mRNA [NM_016109]	NM_016109	Hs.9613	19p13.2
2.165274	GCLC	Hlutamate-cysteine ligase, catalytic subunit	M90656	Hs.654465	6p12
2.1589625	THC2309960	Q7ZX66 (Q7ZX66) RNPC7 protein (Fragment), partial (9%) [THC2309960]		Hs.527551	Xq23
2.150731	THC2269657	Q6QI74 (Q6QI74) LRRG00134, partial (10%) [THC2269657]			chr10
2.1422243	PLXND1	Plexin D1	NM_015103	Hs.301685	3q21.3
2.141769	ABCB6	ATP-binding cassette, sub-family B (MDR/TAP), member 6	NM_005689	Hs.107911	2q36
2.1359584	GSR	Glutathione reductase	NM_000637	Hs.271510	8p21.1
2.119439	A_24_P178167				Xp11.23
2.1153674	AIFM2	Apoptosis-inducing factor, mitochondrion-associated, 2	NM_032797	Hs.655377	10q22.1
2.0789819	KCNMB4	Potassium large conductance calcium-activated channel, subfamily M, β member 4	NM_014505	Hs.525529	12q

Table IV. Downregulated genes following treatment with 15d-PGJ_2 in HHUA cells.

Fold change	Gene symbol	Description	GenBank	UniGene	Map
0.01	FERD3L	Fer3-like (*Drosophila*)	NM_152898	Hs.592168	7p21.1
0.025915636	A_24_P922893				7q11.21
0.027622959	AGR3	Anterior gradient homolog 3 (*Xenopus laevis*)	NM_176813	Hs.100686	7p21.1
0.038513284	MRPL37	Mitochondrial ribosomal protein L37	NM_016491	Hs.584908	1p32.1
0.05087885	NOS2A	Nitric oxide synthase 2A (inducible, hepatocytes)	NM_000625	Hs.434386	17q11.2-q12
0.095559224	C18orf23	Chromosome 18 open reading frame 23	AK091537	Hs.501114	18q21.1
0.10365046	ENST00000329610	Homo sapiens prepro-NPW mRNA for prepro-Neuropeptide W polypeptide, partial cds. [AB084276]		Hs.233533	16p13.3
0.12478433	CASC1	Cancer susceptibility candidate 1	NM_018272	Hs.407771	12p12.1
0.14965945	THC2368014	AY320849 immunoglobulin κ chain variable region (*Homo sapiens*), complete [THC2368014]			2p11.2
0.15056583	WBSCR19	Williams Beuren syndrome chromosome region 19	NM_175064	Hs.645483	7p13
0.15237725	KIAA1183	KIAA1183 protein	AB033009	Hs.7193	19q13.32
0.16197103	A_24_P932355				19p13.11
0.1684146	THC2280638	RL2A_HUMAN (P46776) 60S ribosomal protein L27a, partial (24%) [THC2280638]			4q13.3
0.16913189	AK022268	CDNA FLJ12206 fis, clone MAMMA1000941	AK022268	Hs.658369	3
0.17584784	GAL3ST3	Galactose-3-*O*-sulfotransferase 3	NM_033036	Hs.208343	11q13.1
0.18523274	TMEM169	Transmembrane protein 169	NM_138390	Hs.334916	2q35
0.18725868	THC2441492	ALU7_HUMAN (P39194) Alu subfamily SQ sequence contamination warning entry, partial (12%) [THC2441492]			19q13.12
0.19028467	ENST00000304181	GB|AJ009794.1|CAA08833.1 proline rich domain [NP101191]			10q24.31
0.20250778	PDPR	Pyruvate dehydrogenase phosphatase regulatory subunit	NM_017990	Hs.655245	16q22.1
0.21064165	THC2283809				10q24.1
0.21432775	ZNF791	Zinc finger protein 791	NM_153358	Hs.522545	19p13.2-p13.13
0.21798867	C3AR1	Complement component 3a receptor 1	NM_004054	Hs.591148	12p13.31
0.2198143	CCDC110	Coiled-coil domain containing 110	NM_152775	Hs.41101	4q35.1
0.2209758	KCNAB1	Potassium voltage-gated channel, shaker-related subfamily, β member 1	BC043166	Hs.654519	3q26.1
0.22387888	CHAD	Chondroadherin	NM_001267	Hs.97220	17q21.33
0.22510499	ICAM4	Intercellular adhesion molecule 4 (Landsteiner-Wiener blood group)	NM_001544	Hs.631609	19p13.2-cen
0.22763024	eIF4E	Eukaryotic translation initiation factor 4E	BM981574	Hs.249718	4q21-q25
0.2376016	XPNPEP1	X-prolyl aminopeptidase (aminopeptidase P) 1, soluble	NM_020383	Hs.390623	10q25.3
0.23924729	CPXM1	Carboxypeptidase X (M14 family), member 1	NM_019609	Hs.659346	20p13-p12.3
0.24067116	NDRG2	NDRG family member 2	NM_201535	Hs.525205	14q11.2

Table IV. Continued.

Fold change	Gene symbol	Description	GenBank	UniGene	Map
0.2438523	A_24_P916853			8q24.21	
0.24945486	FLJ21272	Hypothetical protein FLJ21272	AK024925	Hs.612891	1q21.2
0.25685737	CSNK1G1	Casein kinase 1, γ 1; *Homo sapiens* casein kinase 1, γ 1 (CSNK1G1), mRNA	NM_001011664	Hs.254335	15q22.1-q22.31
0.2718289	CATSPER1	Cation channel, sperm associated 1	NM_053054	Hs.189105	11q12.1
0.27470103	APOA4	Apolipoprotein A-IV	NM_000482	Hs.591940	11q23
0.2767344	MMP1	Matrix metallopeptidase 1 (interstitial collagenase)	NM_002421	Hs.83169	11q22.3
0.29412216	C15orf37	Chromosome 15 open reading frame 37	NM_175898	Hs.512015	15q25.1
0.3019541	COPZ2	Coatomer protein complex, subunit ζ 2	NM_016429	Hs.408434	17q21.32
0.3044736	RREB1	Ras responsive element binding protein 1	NM_002955	Hs.298248	6p25
0.31109598	GMFG	Glia maturation factor, γ	NM_004877	Hs.5210	19q13.2
0.3145231	MGC16121	Hypothetical protein MGC16121	BC007360	Hs.416379	Xq26.3
0.31809595	MCCD1	Mitochondrial coiled-coil domain 1	NM_001011700	Hs.558922	6p21.33
0.3269747	WBSCR27	Williams Beuren syndrome chromosome region 27	NM_152559	Hs.647042	7q11.23
0.33880442	DHRS2	Dehydrogenase/reductase (SDR family) member 2	NM_182908	Hs.272499	14q11.2
0.342074	MDFI	MyoD family inhibitor	NM_005586	Hs.520119	6p21
0.3541897	DHRS2	Dehydrogenase/reductase (SDR family) member 2	NM_182908	Hs.272499	14q11.2
0.361466	IFP38	*Homo sapiens* IFP38 (IFP38), mRNA [NM_031943]	NM_031943	Hs.513128	chr13
0.36588448	ENST00000329078	*Homo sapiens*, Similar to spinster-like protein, clone IMAGE:4814561, mRNA, partial cds. [BC041772]		Hs.556015	17p13.2
0.36866197	THC2433384	ALU7_HUMAN (P39194) Alu subfamily SQ sequence contamination warning entry, partial (15%) [THC2433384]			17p13.1
0.37413767	BG182941	Transcribed locus	BG182941	Hs.635280	7

Table V. Permutation analysis of the correlation between GO terms and upregulated genes following treatment with 15d-PGJ$_2$.

GO Accession	GO Term	Corrected P-value	Count in selection
GO:0055114	Oxidation reduction	5.08E-05	10
GO:0016491	Oxidoreductase activity	5.08E-05	10
GO:0005829	Cytosol	3.99E-04	13
GO:0051186	Co-factor metabolic process	0.001967945	5
GO:0016209	Antioxidant activity	0.001967945	4

Genes	GO Term	ID	Treatment/control
GO:0055114	Oxidation reduction		
AKR1C1		A_23_P257971	17.29906688
AKR1C3		A_23_P138541	15.00240358
HMOX1		A_23_P120883	5.318975127
TXNRD1		A_23_P204581	4.005567769
GO:0016491	Oxidoreductase activity		
AKR1C1		A_23_P257971	17.29906688
AKR1C3		A_23_P138541	15.00240358
HMOX1		A_23_P120883	5.318975127
TXNRD1		A_23_P204581	4.005567769
GO:0005829	Cytosol		
AKR1C1		A_23_P257971	17.29906688
HMOX1		A_23_P120883	5.318975127
TXNRD1		A_23_P204581	4.005567769
GCLM		A_23_P103996	3.688437908
GO:0051186	Co-factor metabolic process		
AMBP		A_23_P256504	5.657345747
HMOX1		A_23_P120883	5.318975127
GCLM		A_23_P103996	3.688437908
GCLM		A_32_P177953	3.255236172
GO:0016209	Antioxidant activity		
TXNRD1		A_23_P204581	4.005567769
SRXN1		A_23_P320113	3.1590489
GSR		A_32_P31618	2.458848635
PRDX1		A_23_P11995	2.077957762

binding combined with PI labeling was performed for the distinction of early apoptotic (Annexin V^+/PI^-) and necrotic (Annexin V^+/PI^+) cells. At increasing doses of 15d-PGJ$_2$, a simultaneous increase in both the Annexin V^+/PI^- fraction (early apoptotic) and Annexin V^+/PI^+ (regarded as necrotic) subpopulations was detected (Table II).

Loss of MTP in response to treatment with 15d-PGJ$_2$. It has been shown that the loss of MTP occurs prior to nuclear condensation and caspase activation and is linked to cytochrome *c* release in many, but not all, apoptotic cells (14,15). It was found that the treatment of endometrial cancer cells with 15d-PGJ$_2$ resulted in the loss of MTP (Table II).

Differential gene expression in 15d-PGJ$_2$-treated cells. In order to identify potential and novel target genes responsive to the anticancer effects in 15d-PGJ$_2$-treated endometrial cancer cells, we examined the global changes in gene expression in the HHUA cells following treatment with 10 μM of 15d-PGJ$_2$ for 48 h (Tables III and IV). Of the 44,000 genes, GO analysis was carried out on the genes upregulated and downregulated by the treatment (Tables V and VI).

Effects of 15d-PGJ$_2$ on the expression of novel proteins. To elucidate the common mechanism of action of 15d-PGJ$_2$ in endometrial cancer, we examined the effects of 15d-PGJ$_2$ on the expression of 20 proteins that were selected from the cDNA microarray data in 3 endometrial cancer cell lines using western blot analysis (Fig. 2 and Table VII). 15d-PGJ$_2$ markedly upregulated the levels of AKR1C3 and downregulated the levels of AGR3 and NOS2A proteins in all 3 endometrial cancer cell lines.

Table VI. Permutation analysis of the correlation between GO terms and downregulated genes following treatment with 15d-PGJ_2.

GO Accession	GO Term	Corrected P-value	Count in selection
GO:0002675	Positive regulation of acute inflammatory response	0.064905845	2
GO:0010817	Regulation of hormone levels	0.076163195	3
GO:0032101	Regulation of response to external stimulus	0.076163195	3
GO:0002673	Regulation of acute inflammatory response	0.076163195	2
GO:0002790	Peptide secretion	0.07797773	2

Genes	GO Term	ID	Treatment/control
GO:0002675	Positive regulation of acute inflammatory response		
IL6		A_23_P71037	0.404520132
C3		A_23_P101407	0.450077889
GO:0010817	Regulation of hormone levels		
DHRS2		A_23_P321501	0.311235885
IL6		A_23_P71037	0.404520132
EDN1		A_23_P214821	0.461688691
GO:0032101	Regulation of response to external stimulus		
IL6		A_23_P71037	0.404520132
C3		A_23_P101407	0.450077889
EDN1		A_23_P214821	0.461688691
GO:0002673	Regulation of acute inflammatory response		
IL6		A_23_P71037	0.404520132
C3		A_23_P101407	0.450077889
GO:0002790	Peptide secretion		
IL6		A_23_P71037	0.404520132
EDN1		A_23_P214821	0.461688691

Table VII. Results of western blot analysis in the 3 cell lines.

Name	HHUA	Ishikawa	HEC-59
AGR3	↓	↓	↓
AKR1C1	↑	-	↑
AKR1C3	↑	↑	↑
AMBP	↑	↑	NE
C3AR1	-	-	↓
CHAD	↓	↓	NE
FERDL3	↓	-	-
FTL	↑	NE	-
GAL3ST3	↓	↑	↓
GCLM	-	↑	-
HMOX1	↑	-	-
ICAM4	-	↑	NE
KCNAB1	↓	↓	-
MRPL37	↓	NE	NE
NOS2A	↓	↓	↓
p-elF4E	↓	-	NE
PIR	↓	↑	↑
TRIM16	↑	-	-
TXNRD1	↑	↑	-
UGT1A6	↑	↓	↑

↑, Upregulation; ↓, downregulation; -, no change; NE, no expression.

Discussion

In the present study, we demonstrated that 15d-PGJ_2 inhibits cell viability in endometrial cancer cells. The prominent arrest of these cells in the G2/M phase of the cell cycle and the induction of apoptosis likely account for this inhibitory effect, suggesting that 15d-PGJ_2 has anticancer activity.

In order to investigate the molecular mechanisms involved in the effects of 15d-PGJ_2 on the cell cycle arrest and the induction of apoptosis, we investigated the global gene expression profile changes in HHUA endometrial cancer cells following treatment with 15d-PGJ_2. Surprisingly, the expression of PPARγ or angiotensin II type 1 receptor (AT1R) was not altered, although 15d-PGJ_2 has been characterized as a potent PPARγ ligand. To identify novel target genes of 15d-PGJ_2, we focused on some GO terms of the numerous genes upregulated and downregulated by 15d-PGJ_2 treatment in the HHUA cells. GO analysis revealed that oxidation reduction (GO:0055114) and oxidoreductase activity (GO:0016491) were enriched in genes that were overexpressed in the 15d-PGJ_2-treated HHUA cells compared to the untreated HHUA cells. Both GO terms include AKR1C3.

AKR1C3 is a multifunctional enzyme involved in androgen, estrogen, progesterone and prostaglandin metabolism. AKR1C3-mediated steroid metabolism may play a critical role in the maintenance of viable normal and abnormal endometrial

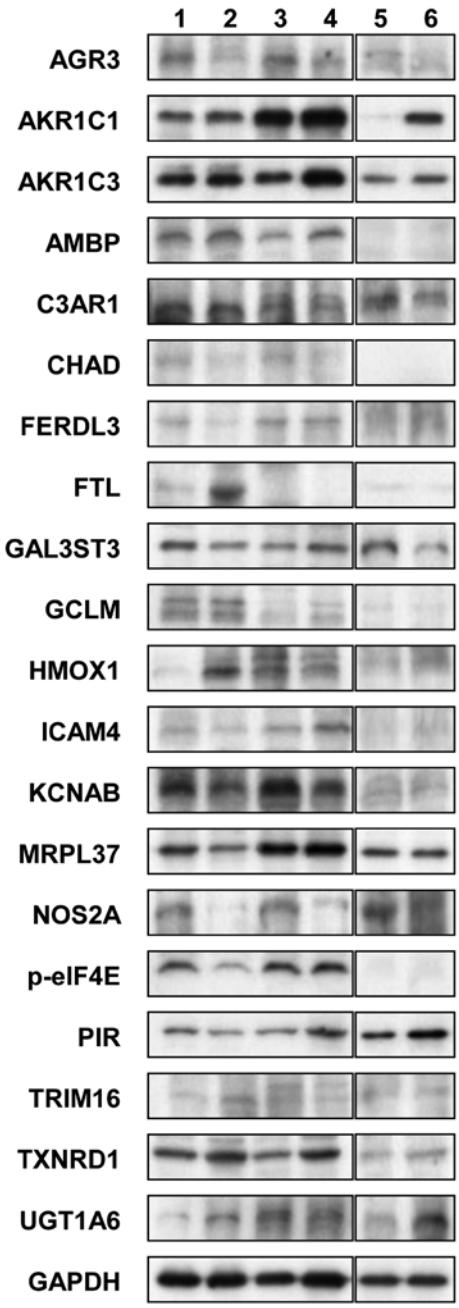

Figure 2. Expression of 20 proteins in endometrial cancer cells measured by western blot analysis. Cells were treated with 10 μM 15d-PGJ$_2$, and cell lysates were harvested after 48 h. Western blot analysis was performed with a series of antibodies. The control cells were treated with the vehicle alone. The amount of protein was normalized by comparison to GAPDH levels. Lane 1, HHUA controls; lane 2, HHUA cells treated with 15d-PGJ$_2$; lane 3, Ishikawa controls; lane 4, Ishikawa cells treated with 15d-PGJ$_2$; lane 5, HEC-59 controls; lane 6, HEC-59 cells treated with 15d-PGJ$_2$.

epithelium (16). AKR1C3 has been reported to play important roles in the physiology of endometrial cells and that suppressed AKR1C3 expression represents a feature that allows the differentiation of hyperplastic and neoplastic endometrial epithelium from normal endometrial epithelium (16). In the present study, we demonstrated that 15d-PGJ$_2$ markedly upregulated the levels of the AKR1C3 protein in all 3 endometrial cancer cell lines. Based on these observations, it can be hypothesized that the 15d-PGJ$_2$-induced anticancer activity may be mediated, at least in part, by the upregulation of AKR1C3 in human endometrial cancer cells.

We confirmed the downregulation of AGR3 using western blot analysis in all 3 cell lines examined. AGR genes, a protein disulfide isomerase (PDI) family, harbour core thioredoxin folds (CxxS motifs) that have the potential to regulate protein folding and maturation. AGR3 is overexpressed by a hormone (estrogen-receptor α)-independent mechanism, identifying a novel protein-folding associated pathway that can mediate resistance to DNA-damaging agents in human cancers (17). These findings indicate that the downregulation of AGR3 by 15d-PGJ$_2$ may cause DNA-damage, leading to the apoptosis of endometrial cancer cells.

Nitric oxide, a reactive free radical, acts as a biological mediator in several processes, including neurotransmission and antimicrobial and antitumor activities. The NOS2A gene encodes a nitric oxide synthase which is expressed in the liver and is inducible by a combination of lipopolysaccharide and certain cytokines. A recent study revealed that NOS2 upregulation contributes primarily to the proliferation and tumor maintenance in highly tumorigenic human glioma stem cells (18). Therefore, our finding that 15d-PGJ$_2$ downregulated NOS2A expression suggests that the eicosanoid may inhibit the proliferation and maintenance of endometrial cancer cells via NOS2A downregulation.

In conclusion, the data from the present study demonstrate that 15d-PGJ$_2$ exhibits anti-proliferative activity, potently induces cell cycle arrest, and stimulates apoptosis in human endometrial cancer cells. These events were accompanied by the upregulation of AKR1C3 and the downregulation of AGR3 and NOS2A. It is suggested that 15d-PGJ$_2$ may be a novel therapeutic option for the treatment of endometrial cancer.

References

1. Reinhardt MJ: Gynecologic tumors. Recent Results Cancer Res 170: 141-150, 2008.
2. Obel JC, Friberg G and Fleming GF: Chemotherapy in endometrial cancer. Clin Adv Hematol Oncol 4: 459-468, 2006.
3. Hill EK and Dizon DS: Medical therapy of endometrial cancer: current status and promising novel treatments. Drugs 72: 705-713, 2012.
4 Ota K, Ito K, Suzuki T, *et al*: Peroxisome proliferator-activated receptor gamma and growth inhibition by its ligands in uterine endometrial carcinoma. Clin Cancer Res 12: 4200-4208, 2006.
5. Xin B, Yokoyama Y, Shigeto T, Futagami M and Mizunuma H: Inhibitory effect of meloxicam, a selective cyclooxygenase-2 inhibitor, and ciglitazone, a peroxisome proliferator-activated receptor gamma ligand, on the growth of human ovarian cancers. Cancer 110: 791-800, 2007.
6. Yang YC, Tsao YP, Ho TC and Choung IP: Peroxisome proliferator-activated receptor-gamma agonists cause growth arrest and apoptosis in human ovarian carcinoma cell lines. Int J Gynecol Cancer 17: 418-425, 2007.
7. Nosjean O and Boutin JA: Natural ligands of PPARgamma: are prostaglandin J(2) derivatives really playing the part? Cell Signal 14: 573-583, 2002.
8. Forman BM, Tontonoz P, Chen J, Brun RP, Spiegeiman BM and Evans RM: 15-Deoxy-delta 12, 14-prostaglandin J$_2$ is a ligand for the adipocyte determination factor PPARγ. Cell 83: 803-812, 1995.
9. Kliewer SA, Lenhard JM, WillsonTM, Patel I, Morris DC and Lehmann JM: A prostaglandin J$_2$ metabolite binds peroxisome proliferator-activated receptor g and promotes adipocyte differentiation. Cell 83: 813-819, 1995.
10. Wang JJ and Mak OT: Induction of apoptosis in non-small cell lung carcinoma A549 cells by PGD$_2$ metabolite, 15d-PGJ$_2$. Cell Biol Int 35: 1089-1096, 2011.

11. Shin SW, Seo CY, Han H, *et al*: 15d-PGJ_2 induces apoptosis by reactive oxygen species-mediated inactivation of Akt in leukemia and colorectal cancer cells and shows in vivo antitumor activity. Clin Cancer Res 15: 5414-5425, 2009.
12. Mansure JJ, Nassim R and Kassouf W: Peroxisome proliferator-activated receptor gamma in bladder cancer: a promising therapeutic target. Cancer Biol Ther 8: 6-15, 2009.
13. Beissbarth T and Speed TP: GOstat: find statistically over-represented Gene Ontologies within a group of genes. Bioinformatics 20: 1464-1465, 2004.
14. Rimon G, Bazenet CE, Philpott KL and Rubin LL: Increased surface phosphatidylserine is an early marker of neuronal apoptosis. J Neurosci Res 48: 563-570, 1997.
15. Chen Y, Kramer DL, Diegelman P, Vujcic S and Porter CW: Apoptotic signaling in polyamine analogue-treated SK-MEL-28 human melanoma cells. Cancer Res 61: 6437-6444, 2001.
16. Zakharov V, Lin HK, Azzarello J, *et al*: Suppressed expression of type 2 3alpha/type 5 17beta-hydroxysteroid dehydrogenase (AKR1C3) in endometrial hyperplasia and carcinoma. Int J Clin Exp Pathol 3: 608-617, 2010.
17. Gray TA, MacLaine NJ, Michie CO, *et al*: Anterior Gradient-3: a novel biomarker for ovarian cancer that mediates cisplatin resistance in xenograft models. J Immunol Methods 378: 20-32, 2012.
18. Eyler C E, Wu Q, Yan K, *et al*: Glioma stem cell proliferation and tumor growth are promoted by nitric oxide synthase-2. Cell 146: 53-66, 2011.